

# Map of distamycin, netropsin, and actinomycin binding sites on heterogeneous DNA: DNA cleavage-inhibition patterns with methidiumpropyl-EDTA·Fe(II)

(DNA sequence determination/intercalation/minor groove binding/daunomycin)

MICHAEL W. VAN DYKE, ROBERT P. HERTZBERG AND PETER B. DERVAN\*

Division of Chemistry and Chemical Engineering, California Institute of Technology, Pasadena, California 91125

Communicated by John J. Hopfield, May 24, 1982

**ABSTRACT** We report a direct technique for determining the binding sites of small molecules on naturally occurring heterogeneous DNA. Methidiumpropyl-EDTA·Fe(II) [MPE·Fe(II)] cleaves double helical DNA with low sequence specificity. Using a combination of MPE·Fe(II) cleavage of drug-protected DNA fragments and Maxam-Gilbert gel methods of sequence analysis, we have determined the preferred binding sites on a *Rsa* I-EcoRI restriction fragment from pBR322 for the intercalator actinomycin D and the minor groove binders netropsin and distamycin A. Netropsin and distamycin A gave identical DNA cleavage-inhibition patterns and bound preferentially to A+T-rich regions with a minimal protected site of four base pairs. We were able to observe the effect of increasing concentration on site selection by netropsin and distamycin A. Actinomycin D afforded a completely different cleavage-inhibition pattern, with 4- to 16-base-pair-long protected regions centered around one or more G·C base pairs.

Many small molecules important in antibiotic chemotherapy bind to double helical DNA (1). Although it is possible to determine the overall affinity and stoichiometry of the noncovalent binding of drugs to DNA, the exact locations and extent of preferred binding sites on naturally occurring heterogeneous DNA sequences are not known. In the case of protein-DNA binding specificity, one useful method for determining protein binding sites on DNA is the DNase inhibition pattern technique, which combines DNase cleavage of protein-protected DNA fragments and Maxam-Gilbert sequence determination methods (2, 3). This useful technique relies on the relatively low specificity of DNase I in a partial digestion and the ability of DNA-bound protein to prevent cleavage of the DNA backbone between the base pairs it covers. The protein-protected DNA sequence is expressed as a gap (light region) in the usually uniform ladder seen in the autoradiogram from a sequence analysis gel revealing the position and extent of the protein binding site (2, 3). This technique has not yet been reported to be useful for small molecules such as drugs important in chemotherapy.

The simple bifunctional molecule, methidiumpropyl-EDTA (MPE) contains the DNA intercalator methidium covalently bound by a short hydrocarbon tether to the metal chelator EDTA (4) (Fig. 1). MPE in the presence of ferrous ion and oxygen efficiently produces single-strand breaks in double helical DNA (4). Using 3' end-labeled DNA restriction fragments from pBR322 plasmid, we have found that MPE is a relatively non-sequence-specific DNA cleaving agent. In effect, MPE·Fe(II) is a small synthetic scissor for DNA that mimics the behavior of DNase and, because of its size, might be a useful tool for probing the locations and extent of binding sites of drugs on naturally occurring DNA.

The publication costs of this article were defrayed in part by page charge payment. This article must therefore be hereby marked "advertisement" in accordance with 18 U. S. C. §1734 solely to indicate this fact.

Actinomycin D, an antitumor antibiotic containing a phenoxazone chromophore and two pentapeptide rings, binds double helical DNA (1). Solution studies are consistent with intercalation as a mode of binding and reveal a preference for guanine-pyrimidine sequences (1, 5-9). Crystallographic studies have provided some insight into the nature of the specific guanine-actinomycin interaction (10, 11).

The antibiotics netropsin and distamycin A are basic oligopeptides containing two and three *N*-methylpyrrole rings, respectively. Netropsin and distamycin A appear to bind in the minor groove of double helical DNA. From solution studies with synthetic polynucleotides, a strong preference for A+T-rich polymers has been shown (12-14). The specificity of distamycin/netropsin binding presumably results from hydrogen bonding between the N-H of the amide linkages of the antibiotic and the potential H-bond acceptor substituents on the A·T base pairs, such as O-2 of thymine and N-3 of adenine (1, 12-16) (Fig. 2).

We report here a direct technique that combines MPE·Fe(II) treatment of drug-protected DNA fragments and Maxam-Gilbert sequence analysis methods to determine the preferred binding sites for the intercalator actinomycin and the minor groove binders netropsin and distamycin A on naturally occurring heterogeneous segments of double helical DNA (Fig. 3). For comparison, the well-characterized anthracycline antitumor antibiotic daunomycin, an intercalator without firm evidence for base composition specificity, was included in this study (1, 17-19).

## MATERIALS AND METHODS

Actinomycin D was obtained from Merck, Sharpe & Dohme. Daunomycin and dithiothreitol were obtained from Calbiochem. Distamycin A was obtained from Boehringer Mannheim. Netropsin was a gift from D. Patel. MPE was synthesized and purified by procedures as described (4).  $\text{Fe}(\text{NH}_4)_2(\text{SO}_4)_2 \cdot 6\text{H}_2\text{O}$  was obtained from Baker.

Solutions of  $\text{Fe}(\text{NH}_4)_2(\text{SO}_4)_2$ , dithiothreitol, and MPE were prepared freshly. MPE was characterized spectroscopically before use. Each reaction mixture (final volume, 10  $\mu\text{l}$ ) contained 10 mM Tris·HCl (pH 7.8), 50 mM NaCl, and  $\geq 600$  cpm of end-labeled [ $^{32}\text{P}$ ]DNA, with the final DNA concentration made up to 100  $\mu\text{M}$  (base pairs) by the addition of sonicated calf thymus DNA. When present, the final MPE concentration was 10  $\mu\text{M}$ ; Fe(II), 10  $\mu\text{M}$ ; and dithiothreitol, 4 mM. Drug concentrations were adjusted as specified in the legend to Fig. 4. A solution of buffered DNA was incubated for 30 min at 20°C with the inhibition drug (either actinomycin D, daunomycin, distamycin, or netropsin). The reaction was initiated by the addition of

Abbreviation: MPE, methidiumpropyl-EDTA.

\*To whom reprint requests should be addressed.

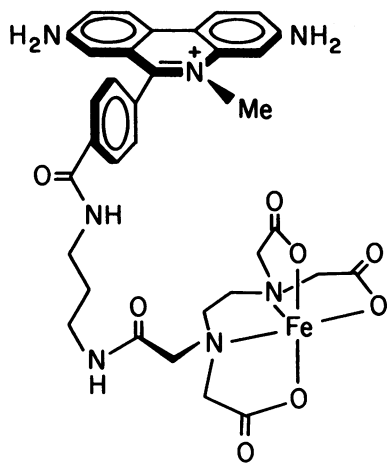


FIG. 1. MPE·Fe(II).

MPE·Fe(II) and dithiothreitol in this order. The reaction was allowed to run at 37°C for 10 min, stopped by freezing in dry ice, lyophilized, and resuspended in formamide loading buffer for gel electrophoresis (20).

**Preparation of Specific Labeled DNA Fragments.** DNA for this investigation was isolated from the bacterial plasmid pBR322 whose entire sequence is known (21). Milligram quantities of the plasmid were grown in *Escherichia coli*, strain HB 101, and isolated by procedures similar to those of Tanaka and Weisblum (22). Superhelical pBR322 plasmids were first digested with the restriction endonuclease *EcoRI* and then 3' end-labeled with [<sup>32</sup>P]dATPs and the Klenow fragment of DNA

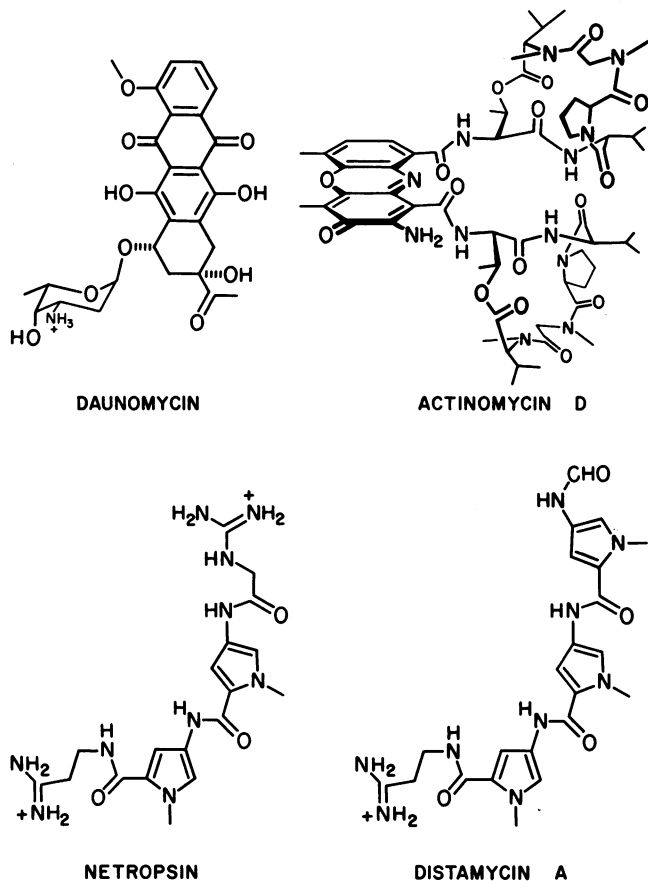


FIG. 2. Antibiotics used to bind to DNA and inhibit cleavage by MPE.

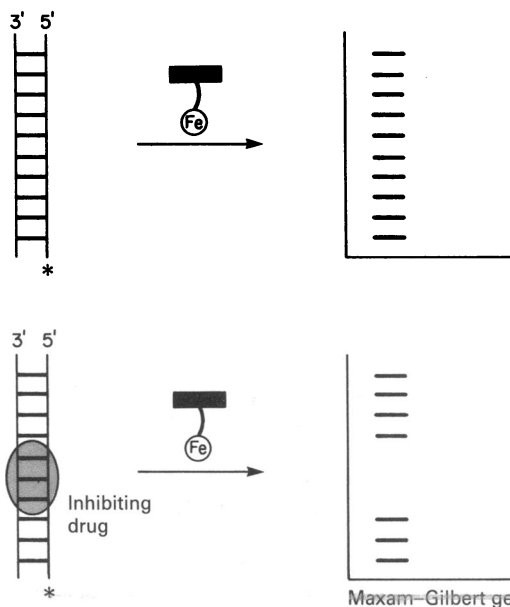


FIG. 3. Illustration of MPE cleavage technique with Maxam-Gilbert gel on natural (Upper) and drug-protected (Lower) segments of double helical DNA.

polymerase I (20). A second enzymatic digest with restriction endonuclease *Rsa I* yielded two end-labeled fragments of 167- and 516-nucleotide lengths. These were isolated by gel electrophoresis on a 5% polyacrylamide, 1:30 crosslinked, 4-mm-thick preparatory gel. Further recovery and purification procedures were similar to those of Maxam and Gilbert (20).

**Sequence Determination Gels.** Resolution of inhibition patterns was achieved by electrophoresis on 0.4-mm-thick, 40-cm-long, 8% polyacrylamide 1:20 crosslinked sequence determination gels containing 50% urea. Electrophoresis was carried out at 1,000 V for 3.5 hr to determine the sequence of 103 nucleotides, beginning 25 nucleotides from the labeled 3' end. Autoradiography was carried out at -50°C without the use of intensification screens.

**Densitometry.** A 20 × 25 cm copy of the original autoradiogram was scanned at 500 nm with the incident beam collimated to a width of 0.1 mm on a Cary 219 spectrophotometer. The data were recorded as absorbance relative to the film base density and analyzed with an Apple microcomputer.

## RESULTS

For an investigation of sequence-specific inhibition of DNA strand cleavage by the antibiotics daunomycin, actinomycin D, distamycin A, and netropsin, a naturally occurring DNA substrate of known sequence was prepared. A 516-base-pair *Rsa I-EcoRI* restriction fragment from the plasmid pBR322 (nucleotides 3847-4363) was chosen. The *EcoRI* site was 3' end-labeled with <sup>32</sup>P. MPE·Fe(II)/dithiothreitol was allowed to react with the 516-base-pair fragment alone and with the 516-base-pair fragment pre-equilibrated with each of the four inhibiting drugs. Cleavage by MPE·Fe(II) was stopped after 10 min by freezing, lyophilization, and resuspension in a formamide buffer. The end-labeled [<sup>32</sup>P]DNA products were analyzed by denaturing 8% polyacrylamide/50% urea gel electrophoresis capable of resolving DNA fragments differing in length by one nucleotide. The autoradiogram data is shown in Fig. 4.

**Control.** Two control experiments in the absence of inhibiting drugs were carried out. The first (Fig. 4, lane 18) was the buffered intact DNA (100 μM in base pairs) in the presence of

10  $\mu\text{M}$  Fe(II) and 4 mM dithiothreitol—concentrations used in all subsequent cleavage-inhibition reactions. The 516-nucleotide-long DNA remained intact, although trace quantities of nicked DNA could be seen that later were shown to result from nonspecific endonuclease activity. The two bands at the top of control lane 18 are presumably the result of incomplete denaturation of the 516-base-pair fragment. The second control (Fig. 4, lane 17) depicted the relatively uniform cleavage pattern generated by MPE (10  $\mu\text{M}$ ) in the presence of Fe(II) (10  $\mu\text{M}$ ) and dithiothreitol (4 mM). This provided the baseline by which other cleavage patterns were then compared. We found it convenient to analyze the data by densitometry (Fig. 5, lane 17).

**Daunomycin.** No pattern was observed with daunomycin inhibition of MPE·Fe(II) cleavage. Samples with increasing concentrations of daunomycin (Fig. 4, lanes 16–14) were allowed

to incubate with the 516-base-pair DNA fragment. Treatment with MPE·Fe(II)/dithiothreitol afforded a uniform cleavage pattern not too different from that of the MPE·Fe(II) control lane. Increasing amounts of daunomycin increased the average length of the cleaved DNA fragment. The highest daunomycin concentration is shown in lane 14, where much of the 516-base-pair fragment remained intact.

**Actinomycin D.** Actinomycin D provided the first evidence for the feasibility of the MPE·Fe(II) inhibition pattern procedure. A series of bands or regions of alternating high and low density on the autoradiogram were observed when MPE·Fe(II)/dithiothreitol cleaved DNA in the presence of actinomycin (Fig. 4, lanes 13–11). The highest concentration of actinomycin D showed the sharpest inhibition patterns (lane 11). The regions of low density, which indicate reduced cleavage by MPE·Fe(II), appeared to be 4–16 nucleotides in length and centered around at least one or more G·C base pairs. The densitometer trace (Fig. 5, lane 11) allowed a measure of the actinomycin blocking of MPE·Fe(II) DNA cleavage on a 103-nucleotide section of the 516-base-pair restriction fragment, illustrated as protected regions on the sequence in Fig. 6, lane 11.

**Distamycin A.** Lower concentrations of distamycin A were sufficient to produce well-resolved inhibition patterns compared to the case of actinomycin D. Certain A+T-rich regions that suffered efficient MPE·Fe(II) cleavage in the presence of actinomycin were protected by distamycin (Fig. 4, light regions on gel lanes 10–8). Inspection of gel lanes 10 and 11 (distamycin and actinomycin, respectively) reveals complementary regions (G+C vs. A+T rich) resulting from different protection by the two drugs (9). We were able to observe the effect of increasing

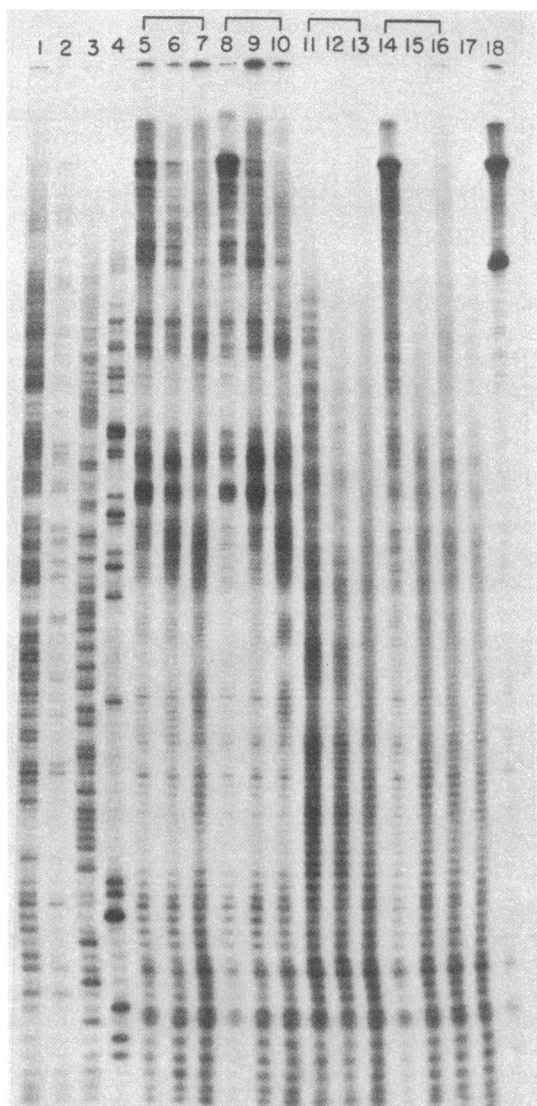


FIG. 4. Autoradiogram of Maxam-Gilbert sequence determination gels. Lanes: 1–4, C+T, C, A>C, and G reactions, respectively (12); 5–18, reactions with 100  $\mu\text{M}$  DNA, 10  $\mu\text{M}$  Fe(II), and 4 mM dithiothreitol; 5–7, reactions with an inhibition drug and 10  $\mu\text{M}$  MPE; 5–7, reactions with netropsin at 230  $\mu\text{M}$ , 23  $\mu\text{M}$ , and 2.3  $\mu\text{M}$ , respectively; 8–10, reactions with distamycin A at 310  $\mu\text{M}$ , 31  $\mu\text{M}$ , and 3.1  $\mu\text{M}$ , respectively; 11–13, reactions with actinomycin D at 325  $\mu\text{M}$ , 32.5  $\mu\text{M}$ , and 3.25  $\mu\text{M}$ , respectively; 14–16, reactions with daunomycin at 150  $\mu\text{M}$ , 15  $\mu\text{M}$ , and 1.5  $\mu\text{M}$ , respectively; 17, reaction with MPE·Fe(II) with no inhibition drug; and 18, reaction with Fe(II) and no MPE or inhibition drug.

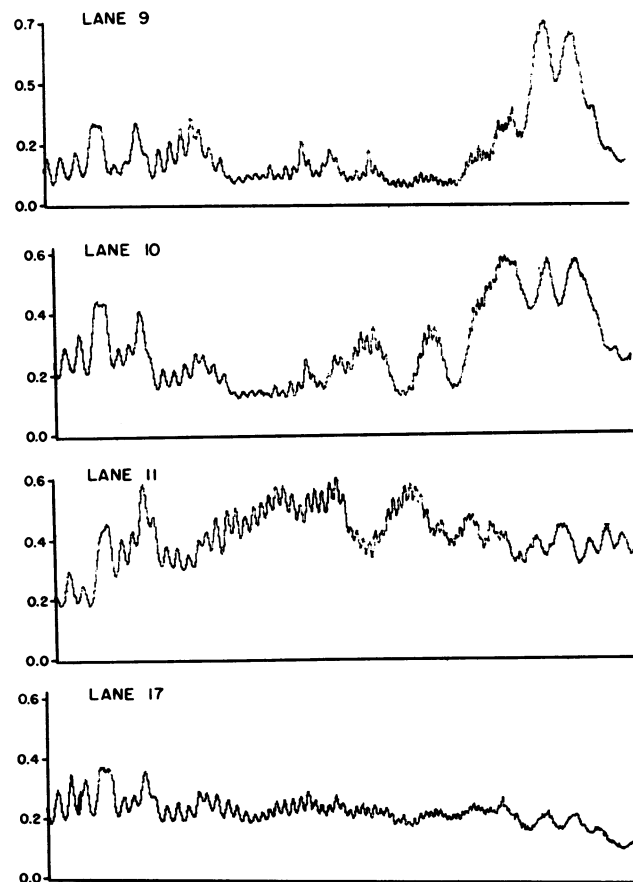


FIG. 5. Densitometer scan left to right corresponds to the bottom to middle of the gel autoradiogram in Fig. 4, lanes 9, 10, 11, and 17. Valleys are drug-protected regions from MPE·Fe(II) cleavage.

concentration on site selection by distamycin A. At low distamycin concentrations, we observed a series of inhibition gaps  $\approx 4$ –16 nucleotides in length—regions rich in A·T base pairs with unprotected spacer regions between them (see Fig. 6, lane 10). As the distamycin concentration was increased, the flanking spacer regions rich in A+T coalesced into one long A+T-rich protected region (lane 11). However, certain sequences containing four or more contiguous G·C base pairs remained unprotected even at the highest concentrations of distamycin.

**Netropsin.** Netropsin, a basic oligopeptide similar in structure to distamycin A, appeared to show the identical inhibition patterns of distamycin A (Fig. 4, lanes 7–5). Not only were the locations and lengths of the various protected regions duplicated, but also the identical coalescence of protected A+T-rich regions at increasing concentrations of netropsin was observed.

**DISCUSSION**

**Cleavage Reactions by MPE·Fe(II).** MPE·Fe(II) was designed and constructed as a non-sequence-specific model of the antitumor antibiotic bleomycin (23, 24). Bleomycin cleaves DNA in a reaction that is dependent on ferrous ion and O<sub>2</sub> at specific sequences (25, 26). The sequence-specific cleavage by bleomycin rules out its effectiveness in generating DNA cleavage-inhibition patterns for small molecules. MPE has low sequence specificity not unexpected from the choice of methidium, an intercalator of low overall base composition specificity (1, 27–29). However, a preference for binding to (3'·5')pyrimidine-purine sequence compared to (3'·5')purine-pyrimidine in deoxyribonucleotides has been established for ethidium (30), as well as a preference for certain conformations of double helical DNA (31).

Addition of reducing agents such as dithiothreitol to solutions of MPE·Fe(II) and DNA enhance the efficiency of the cleavage reaction by 2 orders of magnitude (4). For optimum DNA cleavage-inhibition patterns, we found that fresh dithiothreitol at a concentration in the millimolar range was best. MPE·Fe(II)/base pair ratios were kept in the range of 1:5 to 1:20. Lower concentrations of MPE produced insufficient DNA cleavage, and higher concentrations afforded average DNA lengths too small to provide a satisfactory set of patterns. A MPE·Fe(II)/base pair ratio of 1:10 gave optimal results for the studies described here. Like DNase inhibition patterns, MPE·Fe(II) cleavage of drug-protected restriction fragments is a partial digest, and there is the implicit assumption that a few MPE·Fe(II) strand scissions on the 516-base-pair DNA fragment do not alter the sequence specificity of the inhibiting drug.

The electrophoretic mobilities of fragments generated by MPE·Fe(II) cleavage of 3'-labeled [<sup>32</sup>P]DNA, in the presence or absence of inhibiting drugs, appeared equivalent to those generated by conventional Maxam–Gilbert sequence determination procedures. This implies that the 5' terminus generated by MPE·Fe(II) cleavage is most likely a phosphate group and that, under the denaturing conditions in the sequence assay electrophoresis, the inhibiting drugs are not bound to the DNA. We presume that the reaction responsible for DNA strand scission by MPE·Fe(II) is oxidative cleavage of the deoxyribose ring

analogous to mechanisms postulated for bleomycin activity (23–24).

**Choice of Inhibiting Drugs.** Three of the inhibiting drugs chosen for this test study of MPE·Fe(II) inhibition patterns were known to have sequence preferences, binding site sizes greater than two base pairs, and relatively slow dissociation rates from DNA (1). We do not know yet the importance of size and dissociation rate with regard to the inhibiting drug. For example, although the inability of daunomycin to generate a DNA cleavage-inhibition pattern could be due to a lack of base composition specificity, an alternative explanation is that the binding site size or dissociation rate may be not in a suitable range to provide site-specific protection from MPE·Fe(II) cleavage. Further work must be done to determine the scope and limitations of the MPE inhibition pattern method.

**Interpretation of the DNA Cleavage-Inhibition Pattern.** In principle, an altered DNA cleavage pattern could be the result of suppressed reaction at some sites, enhanced reaction at others, or a combination of both effects. Without ruling out the possibility of enhanced cleavage, we have interpreted the light regions on the autoradiogram as regions of reduced cleavage of DNA by MPE·Fe(II) due to the presence of bound drug. The light regions on the autoradiogram (Fig. 4) correspond to the valleys in the densitometer tracings (Fig. 5), which in turn correspond to the black regions on the 103-base-pair sequence shown in Fig. 6.

We are not yet certain whether there is a one-to-one correspondence of the protected region on one strand of the DNA fragment and the drug binding site. The different accessibility of adjacent deoxyribose rings to the propyl-EDTA·Fe(II) moiety in the unprotected site bound by methidium might result in asymmetric cleavage-inhibition patterns on opposite DNA strands. Most likely the inhibition pattern on each DNA strand is shifted by at least one base pair to the 3' <sup>32</sup>P-labeled side of the drug binding site.

**CONCLUSION**

The results reported here indicate the feasibility of determining the sequence specificity of DNA-binding small molecules on heterogeneous double helical DNA by means of inhibition patterns with DNA-cleaving agent MPE·Fe(II). Antibiotics such as actinomycin D, distamycin A, and netropsin but not daunomycin were observed to generate DNA cleavage-inhibition patterns. These patterns have been sequenced, allowing the location of preferred binding sites of three well-known antibiotics on naturally occurring DNA to be identified. Greater precision in identifying the boundaries of the preferred binding sites will be afforded by an opposite strand analysis (32). Distamycin A and netropsin gave identical results and bound preferentially to A+T-rich regions with a minimal protected site of four base pairs. Coalescence phenomena of certain spacer regions were observed with these minor groove binders at high concentrations. Actinomycin D afforded a completely different inhibition pattern that was 4–16 base pairs long with protected regions centered around one or more G·C base pairs.

With regard to implications for future studies, MPE·Fe(II)



FIG. 6. Illustration of drug-protected regions (black areas) from MPE·Fe(II) cleavage on 103 base pairs of the lower strand of the 516-base-pair fragment. The sequence from left to right corresponds to the bottom to middle of the gel autoradiogram in Fig. 4, lane 11 (actinomycin D at 325  $\mu$ M) and lanes 10 and 9 (distamycin A at 3.1 and 31  $\mu$ M, respectively).

inhibition patterns constitute a rapid technique for assaying hundreds of potential DNA binding sites for antibiotics on one gel. This direct method should prove useful for identifying the preferred sites of DNA-binding small molecules on the native nucleic acid template, which will be necessary for any understanding of the molecular basis of antibiotic action.

We are grateful to the National Institutes of Health for grant support (GM 27681) and a National Research Service Award (GM 07616) to M.W.V. and R.P.H.

1. Gale, E. F., Cundliffe, E., Reynolds, P. E., Richmond, M. H. & Waring, M. J. (1981) *The Molecular Basis of Antibiotic Action* (Wiley, New York), pp. 258–401.
2. Galas, D. J. & Schmitz, A. (1978) *Nucleic Acids Res.* **5**, 3157–3170.
3. Schmitz, A. & Galas, D. J. (1982) in *Methods in DNA and RNA Sequencing*, ed. Weismann, S. (Plenum, New York), in press.
4. Hertzberg, R. P. & Dervan, P. B. (1982) *J. Am. Chem. Soc.* **104**, 313–315.
5. Goldberg, I. H., Rabinowitz, M. & Reich, E. (1962) *Proc. Natl. Acad. Sci. USA* **48**, 2094–2101.
6. Muller, W. & Crothers, D. M. (1968) *J. Mol. Biol.* **35**, 251–290.
7. Krugh, T. R. (1981) in *Topics in Nucleic Acid Structure*, ed. Neidle, S. (Macmillan, London), pp. 197–217.
8. Wells, R. D. & Larson, J. E. (1970) *J. Mol. Biol.* **49**, 319.
9. Patel, D. J., Kozlowski, S. A., Rice, J. A., Broka, C. & Itakura, K. (1981) *Proc. Natl. Acad. Sci. USA* **78**, 7281–7284.
10. Sobell, H. M. (1973) *Prog. Nucleic Acid Res. Mol. Biol.* **13**, 153–190.
11. Takusagawa, F., Dabrow, M., Neidle, S. & Berman, H. M. (1982) *Nature (London)* **296**, 466–469.
12. Luck, G., Treibel, H., Waring, M. & Zimmer, Ch. (1974) *Nucleic Acids Res.* **1**, 503.
13. Zimmer, Ch. (1975) *Prog. Nucleic Acid Res. Mol. Biol.* **15**, 285–318.
14. Wartel, R. M., Larson, J. E. & Wells, R. D. (1974) *J. Biol. Chem.* **249**, 6719–6731.
15. Berman, H. M., Neidle, S., Zimmer, Ch. & Thrum, H. (1979) *Biochim. Biophys. Acta* **561**, 124.
16. Krylov, A. S., Grokhovskiy, S. L., Zasedatelev, A. S., Zhuge, A. L., Gursky, G. V. & Gottikh, B. P. (1979) *Nucleic Acids Res.* **6**, 289.
17. Patel, D. J., Kozlowski, S. A. & Rice, J. A. (1981) *Proc. Natl. Acad. Sci. USA* **78**, 3333–3337.
18. Quigley, G. S., Wang, A. H. J., Ughetto, G., Van Der Marel, G., Van Boom, J. H. & Rich, A. (1980) *Proc. Natl. Acad. Sci. USA* **77**, 7204–7209.
19. Berlin, V. & Haseltine, W. A. (1981) *J. Mol. Biol.* **256**, 4747–4756.
20. Maxam, A. M. & Gilbert, W. (1980) *Methods Enzymol.* **65**, 499–560.
21. Sutcliffe, J. G. (1979) *Cold Spring Harbor Symp. Quant. Biol.* **43**, 77–90.
22. Tanaka, T. & Weisblum, B. (1974) *J. Bacteriol.* **121**, 354–362.
23. Hecht, S. M. L. (1979) *Bleomycin: Chemical, Biochemical and Biological Aspects* (Springer-Verlag, New York).
24. Burger, R. M., Peisach, J. & Horwitz, S. B. (1981) *Life Sci.* **28**, 715–727.
25. D'Andrea, A. D. & Haseltine, W. A. (1978) *Proc. Natl. Acad. Sci. USA* **75**, 3608–3612.
26. Takeshita, M., Grollman, A. P., Ohtsubo, E. & Ohtsubo, H. (1978) *Proc. Natl. Acad. Sci. USA* **75**, 5983–5987.
27. Waring, M. J. (1965) *J. Mol. Biol.* **13**, 269–282.
28. Le Pecq, J.-B. & Paoletti, C. (1967) *J. Mol. Biol.* **27**, 87–106.
29. Muller, W. & Crothers, D. M. (1975) *Eur. J. Biochim.* **54**, 267–277.
30. Kastrup, R. V., Young, M. A. & Krugh, T. R. (1978) *Biochemistry* **17**, 4855–4865.
31. Bresloff, J. L. & Crothers, D. M. (1981) *Biochemistry* **20**, 3547–3553.
32. Van Dyke, M. W. & Dervan, P. B. (1982) *Cold Spring Harbor Symp. Quant. Biol.* **47**, in press.